Eur. Phys. J. D **27**, 15–22 (2003)
DOI: 10.1140/epjd/e2003-00230-6

THE EUROPEAN PHYSICAL JOURNAL D

The dressed states of an electron in a one-dimensional two δ-functions potential

C. Chirilă, M. Boca, V. Dinu, and V. Florescu[a]

Department of Physics, University of Bucharest, Bucharest-Magurele 76900, Romania

Received 1st April 2003
Published online 29 July 2003 –

Abstract. We study, in the framework of the high-frequency Floquet theory, the one-dimensional system consisting of an electron interacting with a symmetric two δ-functions potential in the presence of an intense monochromatic homogeneous electric field. Most of the results concern the attractive case. They include the dependence of the bound states energies of the dressed potential and of some of its resonances positions on the electric field parameter α_0 (the classical free electron quiver motion amplitude) and on the distance between the two centers and the description of the evolution from resonances to laser induced levels *via* two antibound states. The repulsive case is described briefly.

PACS. 32.80.-t Photon interactions with atoms – 32.90.+a Other topics in atomic properties and interactions of atoms with photons – 03.65.Ge Solutions of wave equations: bound states

1 Introduction

In the last 15 years, the unusual atomic behaviour in the presence of high-frequency, high-intensity electromagnetic fields, as predicted by the Floquet theory [1], led to a variety of investigations, most of them theoretical. The most unexpected prediction, found in the framework of high frequency Floquet theory (HFFT), is the phenomenon of stabilization. This phenomenon is the tendency of the atomic system to remains stable against ionization. In the Floquet formalism the stabilization is revealed by the tendency of the imaginary part of the quasienergies to decrease if the intensity of the electromagnetic field is high enough. For a recent review of this subject and the need for further work in the domain of superintense laser-atom physics, we refer to the paper of Gavrila [2].

The results supplied by the Floquet theory prove themselves to be useful for the description of the atoms interaction with not only monochromatic electromagnetic fields introduced adiabatically, but also with shorter ones, if a multicomponent Floquet theory is adopted [3].

In this paper we report our results, based on HFFT, concerning a very simple one-dimensional system, a particle in the potential

$$V(x) = -\frac{\gamma}{2}\left[\delta(x-a)+\delta(x+a)\right], \qquad a>0, \quad (1)$$

subject to the action of a monochromatic electric field described by the vector potential

$$A(t) = A_0 \cos\omega t. \quad (2)$$

All equations and numerical results will be expressed in atomic units.

The HFFT theory, introduced by Gavrila and Kaminski [4], is a limit form of the Floquet theory, corresponding to very high frequency ω and intensity I; from a mathematical point of view, the equations correspond to the limit $\omega \to \infty$, $I \to \infty$, but with a finite value for the ratio

$$\alpha_0 \equiv \frac{\sqrt{I}}{\omega^2}. \quad (3)$$

The quantity α_0 represents the classical free electron quiver motion amplitude in the presence of a plane wave of frequency ω and intensity I. The HFFT limit has already been studied not only for some simple 1D systems [5], but also for realistic systems as the hydrogen atom [6] and the hydrogen molecular ion [7]. The validity of HFFT was analysed in several particular cases, such as the Gaussian potential [8,9], and the one-dimensional δ-function potential [9,10]. It appears that the information obtained from HFFT is useful in more elaborated studies based on exact Floquet calculations.

The electron in the potential (1) and in the absence of the electromagnetic field can be found several times in the literature. It was presented, for instance, as a 1D model for a diatomic ion [11,12]. The most studied problem for the potential (1) was the elastic scattering, including the calculation of transmission and reflection coefficients [13], but also a wavepacket description of the scattering was given, accompanied by a calculation of several resonances [14,15]. Depending on the value of the parameter $\eta \equiv a\,\gamma$, the system has one or two bound states, but, in contrast to other 1D systems studied up to now, it has

[a] e-mail: flor@barutu.fizica.unibuc.ro

a wealthy set of resonances that are relatively close to the real axis for large values of the parameter η.

Recently [16,17], the potential (1) was invoked as a suitable approximation for describing the ground state of a 1D δ-function potential dressed by an external monochromatic electric field.

Most results we present correspond to the attractive case ($\gamma > 0$ in Eq. (1)), but some results corresponding to the repulsive case are present in Sections 2 and 4. In Section 2 we give a brief description of the system in the absence of the electromagnetic field. We use a constant value $\gamma = 2$ and the separation $2a$ between the two points where the δ-functions are located is a parameter we vary in this section and in the following ones. Then, we describe in Section 3 the dressed potential and its bound states as function of the field parameter α_0, defined in (3), for the range $0 \leq \alpha_0 \leq 50$. Section 4 studies the trajectories of several resonances of the dressed potential. Their evolution with increasing α_0 is followed in some detail, illustrating the transition from a resonance to a light induced level, *via* two antibound levels. As it is known [18], beyond the HFFT approximation, the dressed energy levels become quasienergies with a non-zero imaginary part. Our calculation, based on the first correction to HFFT, leads to the results presented in Section 5 for the case of the ground state.

2 The system in the absence of the electromagnetic field

Several results for the system described by the particle under the force derived from (1) for the attractive case, $\gamma > 0$, can be found in the textbook of Galindo and Pascual [19] and in several papers already quoted in the introduction [11–14]. For the purposes of our paper, we describe here the solutions of the time-independent Schrödinger equation.

We write the energy parameter E in Schrödinger equation as $E = k^2/2$. Two values of k are attached to each E, unless a choice is specified.

To each value of E, real or complex, one can attach two solutions, characterized solely by a definite parity and by an "adequate" normalization. At $x = \pm a$ the solutions are continuous and their derivative undergoes a well-defined discontinuity.

For $0 \leq x \leq a$, the even solution $u_0(E;x)$ and the odd solution $u_1(E;x)$ are

$$u_0(E;x) = \cos kx, \quad u_1(E;x) = \frac{1}{k}\sin kx, \quad 0 \leq x \leq a. \tag{4}$$

For $x > a$, they can be written in terms of two exponential functions as

$$u_l(E;x) = C_l^{(+)}(k)\,\mathrm{e}^{\mathrm{i}kx} + C_l^{(-)}(k)\,\mathrm{e}^{-\mathrm{i}kx}, \qquad x > a, \quad l = 0,1. \tag{5}$$

The coefficients, which depend on k and have the property

$$C_l^{(+)}(-k) = C_l^{(-)}(k)\,, \qquad l = 0,1, \tag{6}$$

are the analogues of the 3D Jost functions [20].

In the following, we consider only the solutions (5) in the case $\mathrm{Re}\,k \geq 0$. They will have a *pure outgoing* behaviour at large distances, if, for $x > a$, only the second exponential in (5) will be present, *i.e.*, for

$$C_l^{(-)}(k) = 0, \qquad l = 0,1, \qquad \mathrm{Re}\,k \geq 0. \tag{7}$$

Explicitly written, the conditions take the simple forms

$$2ka = \pm \mathrm{i}\eta\,(\mathrm{e}^{2\mathrm{i}ka} \pm 1)\,, \qquad \eta \equiv a\,\gamma, \tag{8}$$

with the upper and lower sign for the even and odd case, respectively.

The condition can be fulfilled only for discrete sets of values for k, different for the two cases. There are three types of solutions corresponding to

(a) bound states: $k = \mathrm{i}\kappa_b$, $\kappa_b > 0$,
(b) antibound states: $k = -\mathrm{i}\kappa_a$, $\kappa_a > 0$,
(c) resonances (Gamow-Siegert poles): $\mathrm{Im}\,k < 0$, $\mathrm{Re}\,k \neq 0$.

We notice the scaling property

$$E_n(\gamma, a) = \frac{1}{a^2}\,E_n(\eta, 1) = \gamma^2\,E_n(1, \eta), \tag{9}$$

where a label n has been attached to any value of E of the three types of solutions.

For *bound states* one gets, with $k = \mathrm{i}\kappa_b$,

$$2\kappa_b a = \eta\,(1 \pm \mathrm{e}^{-2\,\kappa_b a}). \tag{10}$$

The equation with the upper sign always has a solution, while the equation with the lower sign has a solution only if $\eta \geq 1$. The solution for $\eta = 1$ is in fact $\kappa_b = 0$.

The equation for *antibound states* ($k = -\mathrm{i}\kappa_a$) has no solution in the even case, and has one solution in the odd case, if $\eta \leq 1$.

For further reference, we present in Figure 1 the energy levels E_0 (full thick line, marked by b_0) and E_1 (full thin line, marked by b_1), and the antibound state energy E_a (dashed line, marked by a_1), for the potential strength $\gamma = 2$, as function of the location a. The calculation is done for the electron and the energies are given in Rydbergs. For $a = 2$ and $\gamma = 2$, one finds $E_0(2,2) = 0.517$, which is not far from the binding energy of the hydrogen molecular ion $E_{\mathrm{ion}} = 0.603$. The graph confirms previous results [12, 14]: (i) for $a = 0$ the ground level starts from $E(2,0) = -2$, a value identical to the unique energy level of the single δ-function potential $V(x) = -2\,\delta(x)$, the system to which our system reduces in this case; (ii) the odd level exists only for $\eta \geq 1$ and it starts from 0, its value for $\eta = 1$; (iii) both transcendental equations (10) have the same solution for $a \to \infty$, leading to the energy $E_0(2,\infty) = E_1(2,\infty) = -0.5$. From Figure 1 one sees that a quasidegeneracy of the levels is present for rather low values of a. For $\eta = 1$, the only solution of equation (10) (with the lower sign) for bound states and of the equation for antibound states is $\kappa = 0$, so the antibound and the odd bound state meet at

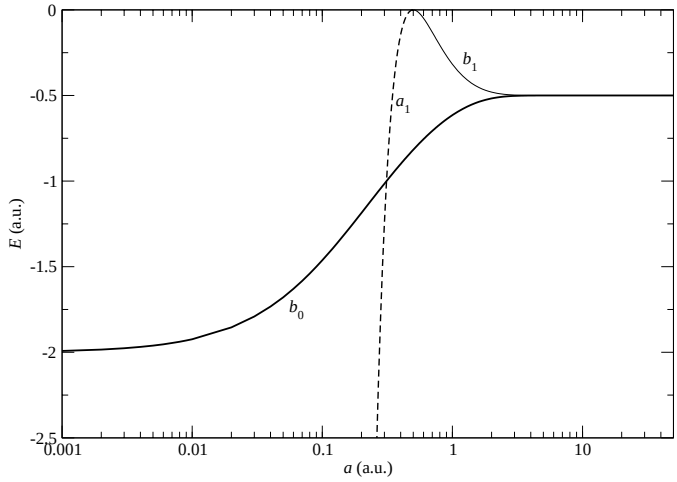

Fig. 1. The energy levels E_0 (full thick line, marked b_0), E_1 (full thin line, marked b_1) and the antibound state energy E_a (dashed line, marked a_1), for the two δ-functions potential (1), with the potential strength $\gamma = 2$, as function of the location a, measured in first Bohr radius. The energies are given in Rydbergs.

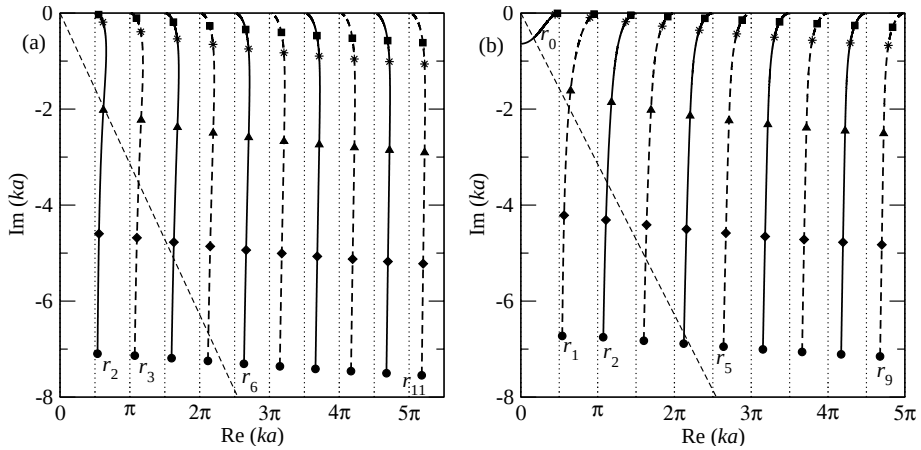

Fig. 2. The trajectories of the first ten Gamow poles in the ka-complex plane. The marked points correspond to $\eta = 10^{-5}$ (circle), $\eta = 10^{-3}$ (diamond), $\eta = 10^{-1}$ (triangle), $\eta = 4$ (star), $\eta = 10$ (square). (a) The attractive case. The poles are denoted by r_n, with $n = 2, \ldots, 11$. (b) The repulsive case. The poles are now denoted by r_n, with $n = 0, \ldots, 9$.

$a = 1/\gamma = 0.5$. With decreasing a, the antibound energy shifts abruptly towards $-\infty$.

The graphs for other values of γ can be obtained from that corresponding to $\gamma = 2$, by the use of the scaling law (9).

The *resonances* are found from the general equations (8). With the notation

$$ka = \alpha - \mathrm{i}\beta\,, \qquad \alpha > 0\,, \quad \beta > 0\,, \tag{11}$$

each of the equations (8) splits into two coupled real equations for α and β:

$$\sin(2\alpha)\,\mathrm{e}^{2\beta} = \mp\,\frac{2\alpha}{\eta}\,, \qquad 1 \pm \cos(2\alpha)\,\mathrm{e}^{2\beta} = -\frac{2\beta}{\eta}\cdot \tag{12}$$

The upper and lower signs correspond to even and odd solutions of the Schrödinger equation, respectively. In both cases, α and β satisfy the equation

$$4(\alpha^2 + \beta^2) - 4\eta\beta = \eta^2(\mathrm{e}^{4\beta} - 1), \tag{13}$$

which is not sufficient to determine them, but which shows that both types of poles are located on the same curve. For $\beta \ll 1$ this curve becomes a portion of a parabola. We shall call the poles even or odd, according to the property of the attached solutions.

For large values of η the solution for α approaches a value from the set $(n-1/2)\,\pi$ in the even case, and a value from the set $n\,\pi$ in the odd case, with n a positive integer. There is only one even pole with $\alpha \in ((n-1/2)\,\pi, n\,\pi))$ and only one odd with $\alpha \in (n\,\pi, (n+1/2)\,\pi))$. For reasons explained later, the resonances will be denoted k_n, starting with $n = 2$.

In Figure 2a we present the trajectories in the complex k-plane of the first ten resonances. The full lines are trajectories of "even" poles, and the dashed ones of "odd" poles. The marked points correspond (from below to top) to values of $10^{-5}, 10^{-3}, 10^{-1}, 4$ and 10 for η, as indicated in the legend. The vertical bars mark multiples of $\pi/2$. We use the convenient variables $\mathrm{Re}\,(k_n\,a)$, $\mathrm{Im}\,(k_n\,a)$. A comparison of our Figure 2a with Figure 1 from [21], corresponding to a family of square wells of variable depths and widths, shows similarities in the tendency of the poles to go to infinity approaching the vertical bars for $\eta \to 0$. For $a = 0$ one gets the case of a one δ-function potential, which has no resonances at all. For $\eta \to \infty$ the resonances reach the real axis at multiples of $\pi/2$.

In the repulsive case ($\gamma < 0$ in Eq. (1)) the resonances are denoted by r_n, with $n = 0, 1, ...$ The attached solutions of the Schrödinger equation have the parity of n. In Figure 2b we present several resonances trajectories in the absence of the field. The first resonance r_0 exists

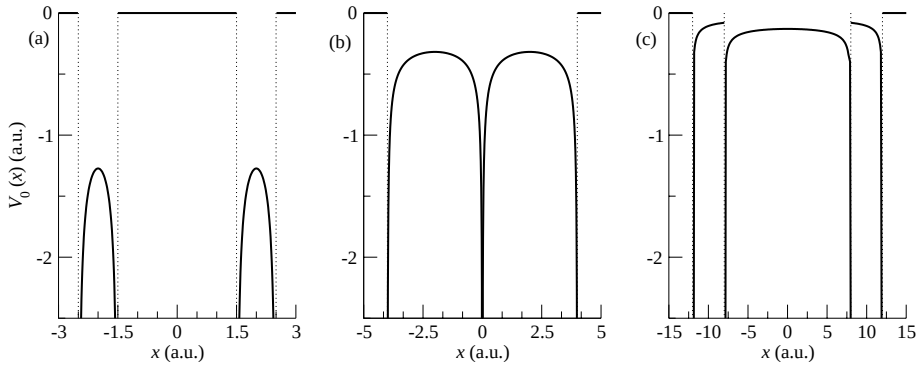

Fig. 3. The dressed potential in equation (15) for $\gamma = 2$ and $a = 2$: (a) $\alpha_0 = 0.5$; (b) $\alpha_0 = 2$; (c) $\alpha_0 = 10$.

only for $\eta > 0.74$. This resonance and its correspondent in the third quadrant meet on the imaginary axis of the complex k-plane at $k = -0.32\,\mathrm{i}$ and generate two antibound states, present for $\eta < 0.74$. The resonance r_n has $n\,\pi/2 < \mathrm{Re}\,(k_n\,a) < (n+1)\,\pi/2$.

3 The dressed potential and its energy levels

In the high-frequency limit of the Floquet theory, the complex quasienergies reduce to real quantities coincident with the energy levels of the particle in the so-called dressed potential $V_0(\alpha_0; x)$, defined as the average on a period T of the translated potential,

$$V_0(\alpha_0; x) = \frac{1}{T}\int_0^T V(x - \alpha_0\,\sin\omega t)\,\mathrm{d}t. \qquad (14)$$

In our case, the dressed potential can be expressed as a sum of two terms, each representing the dressed potential attached to a δ-function potential, located in a or in $-a$,

$$V_0(\alpha_0; x) = V_0^\delta(\alpha_0; x - a) + V_0^\delta(\alpha_0; x + a)\,, \qquad (15)$$

with

$$V_0^\delta(\alpha_0; x) = -\frac{\gamma}{\pi}\frac{1}{\sqrt{\alpha_0^2 - x^2}}\,, \qquad |x| < \alpha_0, \qquad (16)$$

and $V_0^\delta(x) = 0,\ |x| > \alpha_0$.

Figure 3 illustrates the behaviour of the dressed potential for $\gamma = a = 2$ and three values of α_0: 0.5, 2 and 10.

For $\alpha_0 \neq a$, the dressed potential is singular in four points, $x = -a \pm \alpha_0$, $x = a \pm \alpha_0$. For $\alpha_0 < a$, the dressed potential is 0 in three regions of the x-axis: $(-\infty, -a - \alpha_0)$, $(-a + \alpha_0, a - \alpha_0)$ and $(a + \alpha_0, \infty)$. For $\alpha_0 \geq a$, the middle region disappears. For $\alpha_0 = a$, the dressed potential is singular at $x = -2a$, 0 and $2a$. For $\alpha_0 > a$, the three adjacent regions in which the potential is not zero are $(-a - \alpha_0, a - \alpha_0)$, $(a - \alpha_0, -a + \alpha_0)$ and $(-a + \alpha_0, a + \alpha_0)$. Both terms in (15) contribute in the region $(a - \alpha_0, -a + \alpha_0)$.

We notice the following scaling property:

$$E(\gamma, \alpha_0, a) = \gamma^2\,E(1, \alpha_0, \eta). \qquad (17)$$

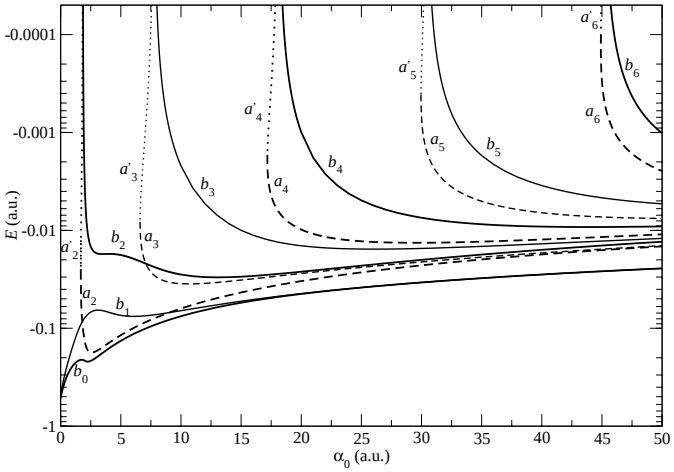

Fig. 4. Bound and antibound levels of the dressed potential for $\gamma = 2$ and $a = 2$: even bound states−full thick lines, odd bound states−full thin lines, even antibound states−thick dashed/dotted lines, odd antibound states−thin dashed/dotted lines.

By integrating the Schrödinger equation attached to (15) we have determined the energy levels for different values of the potential parameter a and $0 < \alpha_0 < 50$. The method of integration is an adaptation of that presented in the case of one δ-function potential [9]. The case $\gamma = a = 2$ is shown in Figure 4, for $0 < \alpha_0 < 50$, representing bound and antibound levels. The curves b_0 and b_1 are the only ones present in the absence of the field. As it is clear from Figure 1, at the values we have chosen for γ and a the two energies are almost equal in the absence of the field. With the increase of α_0 the levels become distinct, then get close again and for $\alpha_0 > 15$ they are practically coincident. The ground level changes monotonically with α_0, except for the vicinity of $\alpha_0 = a$. The graph shows five light induced levels, $b_2, \ldots, b_6$ and ten antibound states, denoted by a_n and a'_n ($n = 2, \ldots, 6$), all light induced. The bound levels with attached even/odd states are represented by full thick/thin lines, the antibound levels a_n and a'_n, with attached even/odd states by dashed thick/thin lines, and dotted thick/thin lines, respectively. The values of α_0 at which the studied light induced levels appear are 1.90, 7.77, 18.12, 30.46 and 45.22. The ten antibound states

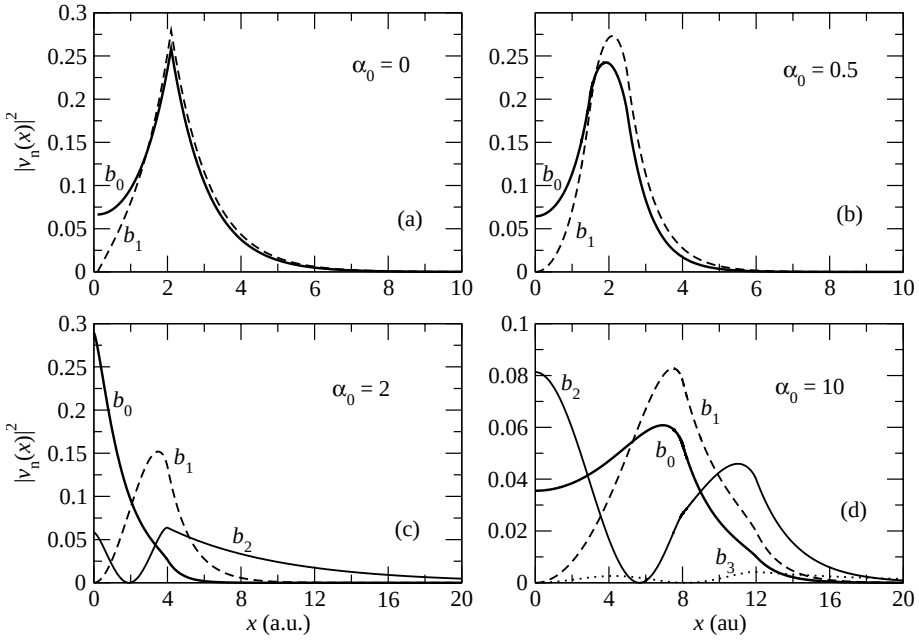

Fig. 5. The probability density of localization in the case $\gamma = 2$ and $a = 2$ for the first four dressed states: (a) $\alpha_0 = 0$; (b) $\alpha_0 = 0.5$; (c) $\alpha_0 = 2$; (d) $\alpha_0 = 10$.

appear at the values 1.67, 6.6, 17.18, 29.95 and 44.91 for α_0. The antibound states denoted by a'_n exist in narrow regions of values of α_0. The antibound states are directly linked with resonances. More about this is explained in Section 3, in connection with Figure 7.

Finally, in Figure 5 we present graphs of the probability density of localization $|v_n|^2$ in the region $0 < x < 20$ for the first four dressed bound states, with v_n the eigenfunction corresponding to the energy E_n. The figures correspond to $\gamma = a = 2$. Figure 5a describes the situation in the absence of the field ($\alpha_0 = 0$), where, as well for $\alpha_0 = 0.5$ in Figure 5b, only the levels b_0 and b_1 exist. The curves in Figure 5a display the discontinuity of the first derivative of the eigenfunction at $x = a$. This discontinuity is not present for the dressed potential eigenfunctions. The behaviour of the maximum of the probability density for the b_0 state follows closely the behaviour of the potential in Figure 3: with increasing α_0 it starts to switch from x close to 2 toward lower values. For $\alpha_0 = 2$ (Fig. 5c) this maximum has reached the origin and the distribution is narrow. For larger values of α_0 the distribution becomes broader; it is shifted toward $\alpha_0 - a$ and another maximum will develop at $\alpha_0 + a$. This second maximum is not visible in Figure 5d corresponding to $\alpha_0 = 10$ (notice the different scale on the vertical axis in Figure 5d compared with the others). At $\alpha_0 = 2$ (Fig. 5c) the light induced level b_2 is present. At $\alpha_0 = 10$ the maximum of b_1 is also practically at $x = \alpha_0 - a = 8$, as that of b_0, and that of b_2 is near $\alpha_0 + a = 12$. In conclusion, the distributions indicate the presence of the singular points of the dressed potential, and one can see the tendency to a polychotomic behaviour of the states. The picture complicates for other light induced states, being influenced by the presence of nodes.

4 The dressed potential resonances

We have determined also several resonances of the dressed potential (15). In Figure 6a we display the trajectory of the first five resonances in the ka-complex plane, in the *attractive case*. We present results for $\gamma = 2$, as we did for the energy levels. The resonances start at $\alpha_0 = 0$ from the positions denoted by a star in Figure 2a, corresponding to $\eta = 4$. The notation r_n, with $n \geq 2$, was adopted in order to have the same index attached to the resonance as to the light induced level it generates for a well defined value of α_0. So, there is no resonance denoted by r_1. The trajectories of the resonances remind of those found for the case of a single δ-function potential [17]. With increasing α_0, the resonances go below the bisectrix of the fourth quadrant and later reach the imaginary axis. Each resonance r_n meets then a pair pole located in the third quadrant, and the two evolve in two antibound levels a_n and a'_n. Then, with further increase of α_0, the antibound level denoted a'_n becomes a bound level and the one denoted a_n remains antibound. This evolution is shown in detail for the first resonance r_2 in the insets of Figure 7.

Figure 6b presents the evolution of resonances $r_0, ..., r_5$ in the *repulsive case*. The starting points, marked by a star, correspond to $\alpha_0 = 0$ and can be found in Figure 2b. Each trajectory ends up in the origin for large values of α_0.

Coming back to the *attractive case*, we present Figure 7. In the main figure the real and imaginary part of the energy of the resonances r_2 to r_6 are represented separately (Figs. 7a and 7b, respectively). With increasing α_0, the real part of each resonance energy decreases, becoming negative. In the case of r_2, the real part of the energy vanishes for $\alpha_0 = 1.51$. The two antibound states replacing the resonance and its pair in the third quadrant

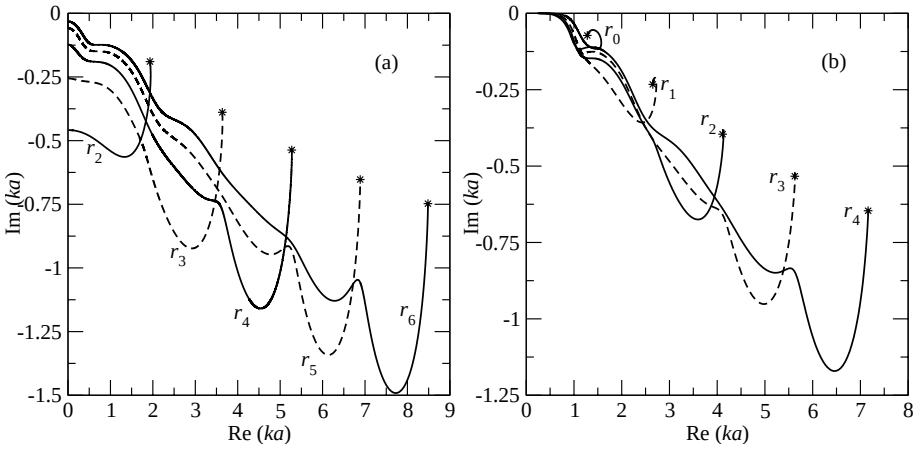

Fig. 6. Trajectories of the even (full line) and odd (dashed line) resonances in the complex plane ka in their dependence of the field parameter α_0, for $\gamma = 2$: (a) the attractive case; (b) the repulsive case.

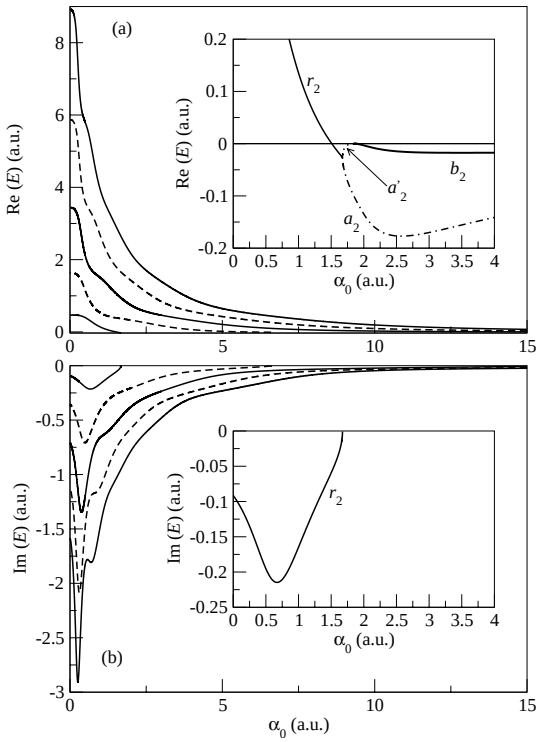

Fig. 7. The dependence of the resonances energy of the parameter α_0. (a) The real part of the resonance energy as function of α_0. (b) The imaginary part of the resonance energy as function of α_0. (Insets) The evolution of the resonance r_2 in two antibound states, one of which becomes the light induced level b_2.

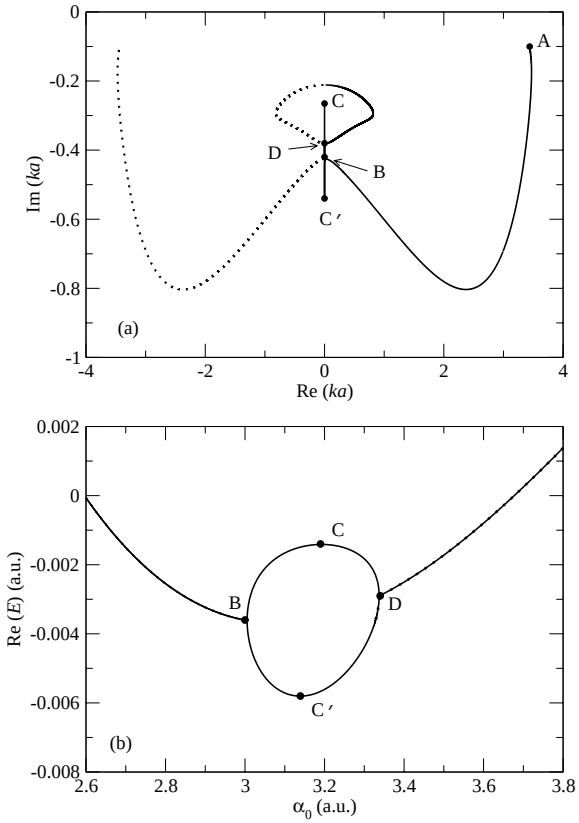

Fig. 8. The resonance r_3 and its pair in the case $\gamma = 2$ and $a = 5$. (a) The trajectory in the complex k-plane. (b) The real part of the energy in the range $2.6 \leq \alpha_0 \leq 3.8$.

appear for $\alpha_0 = 1.67$ and coexist until $\alpha_0 = 1.84$ when the antibound level a_2' becomes the energy level b_2.

We have studied also the changes in the resonances trajectories connected with the increase of the two δ-functions separation. At $a = 5$ we have found resonance trajectories similar to those in Figure 5, with one exception, the trajectory of the resonance r_3. In order to describe it, we present Figure 8. In Figure 8a the trajectory is shown in the k-plane. Starting from the point A, corresponding to $\alpha_0 = 0$, the trajectory approaches the imaginary axis of the k-plane and reaches it at $\alpha_0 = 3$. There it meets the pair pole from the third quadrant and two antibound states move, one first upward (from B to C), then downward (from C to D), the other one first downward from B to C′, then up to D. From D, the poles leave the imaginary axis. The resonance pole reaches again the imaginary axis at $\alpha_0 = 6.7$ where, finally, it becomes a light induced antibound state. Figure 8b displays the behaviour of the real part of the resonance energy $k_3^2/2$ in the

range (2.6, 3.8) for α_0. At $\alpha_0 = 2.6$ the resonance reaches the bisectrix of the fourth quadrant, so the real part of the energy vanishes. Then it takes negative values. The resonance energy is real between the points B and D, where the resonances at E and E^* (* means complex-conjugate) are replaced by antibound states. Then, up to $\alpha_0 = 3.68$, the resonance is below the bisectrix of the fourth quadrant. The evolution after crossing it is that represented in Figure 8b.

5 The width of the dressed ground state level

The results given by the equations of HFFT can be improved by calculating successive corrections given by the iterative procedure developed by Gavrila [18]. In the first order, the energy levels undergo a shift and acquire a width. The width of a level depends not only of α_0, but also on the frequency ω. The width of a dressed level denoted by E_n is [18]

$$\Gamma_n^{\mathrm{HF}} = \sum_{N=1}^{\infty} \Gamma_{N,n}^{\mathrm{HF}} = 2\pi \sum_{N=1}^{\infty} \int_{-\infty}^{\infty} \delta(k^2/2 - N\omega - E_n) \times |\langle v_n | V_N | \Phi(k) \rangle|^2 \, \mathrm{d}E, \quad (18)$$

with V_N the Fourier components of the translated potential, v_n the energy eigenfunction attached to E_n, and $|\Phi(k)\rangle$ the continuum energy eigenfunction corresponding to the energy $E = k^2/2$, normalized in the energy scale.

We refer here only to the ground state width, presenting it in Figure 9, as function of α_0, for the case $a = 2$ and two frequencies, $\omega = 2$ and $\omega = 4$. The full curves correspond to a number $N_{\max} = 120$ for $\omega = 2$, and $N_{\max} = 100$ for $\omega = 4$ terms included in the series (18), and the dashed curves represent the partial width $\Gamma_{1,1}^{\mathrm{HF}}$.

The behaviour of Γ_1^{HF} illustrates the quasistationary (adiabatic) stabilization, as defined in [2]: a decrease in an oscillatory manner after a critical value of α_0.

We have investigated to what extent Born approximation is valid for the partial widths. In Born approximation the continuum energy eigenfunction is replaced by a plane wave. A comparison of the numerical value of $\Gamma_{1,N}^{\mathrm{HF}}$ with its Born approximation indicates that for $N > 10$ at $\omega = 2$ one can safely use the Born approximation for the partial widths. At larger values of ω the agreement was found for even smaller values of N ($N = 8$ for $\omega = 4$).

6 Conclusion

In this paper we have reported the results of a systematic study of solutions of the Schrödinger equation for the dressed symmetric two δ-functions potential, attractive or repulsive, in the range $0 \leq \alpha_0 \leq 50$ of the external field parameter α_0 defined in equation (3). The evolution of the energy levels and of a number of resonances with the increasing of α_0 was followed in detail. We have presented examples of the evolution from a resonance to a bound state, as the mechanism for the apparition of light induced states. As in the case of the one δ-function potential we have studied previously [17], the apparition of a light induced state is preceded by the existence of two antibound states, one of which exists only in a small region of values of α_0, extended from the value at which the resonance meets its pair pole and two antibound states emerge to the value corresponding to the LIS apparition. For the ground state we have illustrated the tendency of the wavefunction to a polychotomic behaviour, and we have calculated the width.

The results could serve as a guide in a study based on Floquet theory beyond the HFFT approximation.

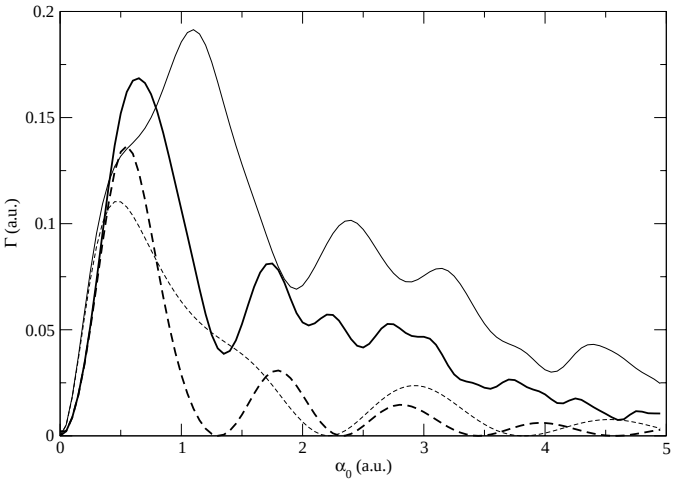

Fig. 9. The total width Γ_1^{HF} and the partial width $\Gamma_{1,1}^{\mathrm{HF}}$ of the level E_0 for the frequencies $\omega = 2$ (full thin line−total width, dashed thin line−partial width) and $\omega = 4$ (full thick line−total width, dashed thick line−partial width).

One of the authors (C.C.) is grateful to the World Federation of Scientists for a Romanian National Scholarship Program grant. M.B. thanks the Romanian Horia Hulubei foundation for financial support. This work was partially supported by CNCSIS, the Romanian Scientific Research Council for Higher Education, grant 146/2002.

References

1. *Atoms in Intense Fields*, edited by M. Gavrila (Academic Press, New York, 1992)
2. M. Gavrila, J. Phys. B: At. Mol. Phys. **35**, R147 (2002)
3. J.C. Wells, I. Simbotin, M. Gavrila, Phys. Rev. A **56**, 3961 (1997); H.C. Day, B. Piraux, R.M. Potvliege, Phys. Rev. A **61**, 031402-1(R) (2000)
4. M. Gavrila, J.Z. Kaminski, Phys. Rev. Lett. **52**, 613 (1984)
5. T.P. Grozdhanov, P.S. Krstic, M.H. Mittlemann, Phys. Lett. A **149**, 144 (1990)
6. M. Pont, M. Gavrila, Phys. Lett. A **123**, 469 (1987)

7. J. Shertzer, A. Chandler, M. Gavrila, Phys. Rev. Lett. **73**, 2039 (1994)
8. M. Marinescu, M. Gavrila, Phys. Rev. A **53**, 2513 (1996)
9. M. Stroe, M. Boca, V. Dinu, V. Florescu, Laser Phys. (accepted, 2003)
10. M. Dörr, R.M. Potvliege, J. Phys. B **33**, L233 (2000)
11. A.A. Frost, J. Chem. Phys. **25**, 1150 (1956)
12. I. Richard Lapidus, Am. J. Phys. **38**, 905 (1970)
13. D. Lessie, J. Spadaro, Am. J. Phys. **54**, 909, (1986)
14. C.L. Hammer, T.A. Weber, V.S. Zidell, Am. J. Phys. **45**, 933 (1977)
15. S.H. Patil, A.S. Roy, Phys. Scripta A **253**, 517 (1998)
16. Jan Mostowski, J.H. Eberly, J. Opt. Soc. Am. B **8**, 1212 (1991)
17. M. Boca, C. Chirilã, M. Stroe, V. Florescu, Phys. Lett. A **286**, 410 (2001)
18. M. Gavrila, in *Atoms in Intense Fields*, edited by M. Gavrila (Academic Press, New York, 1992), p. 435
19. A. Galindo, P. Pascual, *Quantum Mechanics* (Springer Verlag, Berlin, 1990), Vol. I
20. C.J. Joachain, *Quantum Collision Theory* (North-Holland, Amsterdam, 1987)
21. H.M. Nussenzveig, Nucl. Phys. **11**, 499 (1959)